J Mater Sci (2011) 46:7144–7151
DOI 10.1007/s10853-011-5437-4

SIZE DEPENDENT EFFECTS

Structure sensitivity of methanol decomposition on Ni/SiO_2 catalysts

Mihail Mihaylov · Tanya Tsoncheva · Konstantin Hadjiivanov

Received: 17 December 2010 / Accepted: 2 March 2011 / Published online: 11 March 2011

Abstract Three different silica-supported nickel samples were prepared by successive adsorption, reduction, and passivation (SARP) of nickel. The materials obtained were characterized by various techniques (TEM, XRD, H_2 chemisorption, FTIR spectroscopy of adsorbed CO, FMR). Metal nickel particles were uniformly distributed by size with all samples. With increasing the number SARP cycles (1, 3, and 5, respectively) the metal concentration (3.6, 7.6, and 12.6 wt%, respectively) and the mean particle size (4–5, ca. 6 and ca. 7 nm, respectively) also increased without substantial increase of the number of metal particles. The samples were tested as catalysts in methanol decomposition to CO and H_2. It was found that this reaction was structure sensitive and the turn-over frequency decreased with the particle size increase. In contrast, the secondary interaction between the reaction products, i.e., CO methanation (occurring above 515 K) appears to be structure insensitive.

Introduction

The particle size effect in catalysis is a well-known phenomenon [1, 2]. Most often the so-called turn-over frequency (TOF) defined as the average activity per catalytic site, is used to compare catalytic performance [2, 3]. Reactions on metal nanoparticles can be classified as structure sensitive and structure insensitive. With structure insensitive reactions TOF does not depend on the particle size. Structure sensitive reactions require specific grouping of atoms on the surface and their population vary with particle size. As a result, they are strongly affected by the metal particle size. The achievements on the structure sensitivity up to 1989 are summarized in the excellent review of Che and Bennett [2]. However, despite of the fact that "nanocatalysis" has recently attracted much interest [4], there is not substantial development of the topic in the recent years. Here, the works of Hou et al. [5, 6] should be mentioned. These authors investigated a series of different-sized (4.5–45.0 nm) 5 wt% Ni catalysts in methane autothermal reforming with CO_2 and O_2 [5] and in partial oxidation of coke oven gas [6] and established structure sensitivity: small sized nickel particles were more efficient.

Owing to the difficulties in the preparation of uniformly distributed small metal particles with pre-set size, the available unambiguous data on structure sensitive reactions are restricted. It was demonstrated that adsorption of metal cations on oxides followed by reduction is a promising method for preparation of relatively homogeneously distributed small metallic particles [2, 7, 8]. A disadvantage of this technique is that metal loading is restricted by the number of specific sites on the support surface where adsorption of cations occurs. However, in the previous studies the authors demonstrated that reduction of Ni^{2+} [9] or Pt^{n+} ions [10] adsorbed on titania led to formation of metal particles and simultaneous liberation of original adsorption sites. This allowed performance of a subsequent adsorption-reduction cycle which led to increase in the metal content and the mean particle size.

Because of the high-reduction temperature of titania-grafted nickel, the metal particles were covered by sub-oxide support phase (the so-called SMSI effect [11]). This hindered the studies of structure sensitive catalytic

M. Mihaylov (✉) · K. Hadjiivanov
Institute of General and Inorganic Chemistry, Bulgarian Academy of Sciences, 1113 Sofia, Bulgaria
e-mail: misho@svr.igic.bas.bg

T. Tsoncheva
Institute of Organic Chemistry with a Centre of Phytochemistry, Bulgarian Academy of Sciences, 1113 Sofia, Bulgaria

reactions. Therefore, the authors looked for a system for which SMSI was not typical. Analysis of literature data indicated that silica is probably the best support choice. A problem in this case was reoxidation of nickel between the adsorption–reduction cycles that resulted in re-blocking of part of the adsorption sites [12]. To restrict this process, it was applied passivation of the metal particles after each reduction in a flow of 1% oxygen in argon [13]. In this study the authors report results on the characterization of a series of Ni/SiO_2 catalysts prepared by successive adsorption–reduction–passivation and their catalytic behavior in methanol decomposition to H_2, CO, and methane.

During the last two decades methanol decomposition has been intensively studied as a source of alternative clean and efficient fuel for vehicles, gas turbines, and fuel cells [14–17]. Because of the high endothermicity of the process, it has attracted growing interest for the recovering of waste heat from exhausted gases as well. The CO methanation, which is also described as a second stage of interaction between the CO and H_2 products of methanol decomposition, gains a considerable interest in various industrial processes, including the removal of CO and CO_2 in the feed gas for the ammonia synthesis [18], in connection with gasification of coal, where it can be used to produce methane from synthesis gas [19], and in relation to Fischer–Tropsch synthesis [20].

Methanol decomposition is also a good test reaction because gives the opportunity to study metal catalysts simultaneously in two different processes: (i) the basic reaction, i.e., methanol decomposition to H_2 and CO and (ii) the secondary reaction, i.e., methanation of CO. If the dependence of TOF on metal particle size is different for the two reactions, at least one of them is structure sensitive. That is why the authors have chosen this process to test the supported nickel catalysts. There is no consensus in the literature about the structure sensitivity of methanation reaction. According to Goodman et al. [21], methanation is a classical example of structure insensitive reaction. It was concluded that this process proceeded with comparable rates per Ni atom on single crystal and supported nickel [22]. However, according to the review of Che and Bennett [2] an antipathetic structure sensitivity (i.e., TOF increases with the particle size) was demonstrated in many cases. Recent data also indicated that the methanation reaction is structure sensitive and it is suggested that low-coordinated atoms (e.g., on steps) play important role as catalytically active sites [23, 24]. Methanol decomposition to CO and H_2 on nickel catalysts is less studied in this respect. It was reported [16, 17] that methanol decomposition to CO and H_2 proceeded with higher rate on well-crystallized nickel particles. The authors [17] speculated that the catalytically active site was constituted by two nickel atoms, each of them being able strongly to adsorb hydrogen or carbon monoxide.

In this article the authors (i) demonstrate the ability of the preparation method elaborated by us to produce series of samples of well-defined nickel nanoparticles with a preset size and (ii) report on the structure sensitivity of methanol decomposition.

Experimental

Catalyst preparation

The silica support used was a commercial *Aerosil* sample with a specific surface area of 336 $m^2\ g^{-1}$.

Solution of Ni^{2+} (0.3 M) was prepared from $Ni(NO_3)_2$ and ammonia (final NH_3 concentration of 12.5%). To adsorb Ni^{2+} ions, 10 g of SiO_2 were suspended in 150 mL of this solution and agitated for 1 h. Then the precipitate was filtered, washed thoroughly with water, dried and calcined for 1 h at 623 K.

Second adsorption of Ni^{2+} was performed in the same way, but in this case a reduced and passivated catalyst obtained by the first grafting was used instead of the pure support. All other procedures were as the described for the first adsorption. Each next adsorption was performed in analogous way.

Reduction of the samples was performed at 973 K by H_2 with a flow rate of 50 mL min^{-1}. The temperature was attained with a heating rate of 5 K min^{-1}. After 1 h reduction the samples were cooled to ambient temperature in the hydrogen flow and then passivated. The passivation was performed at ambient temperature in a flow of 1 vol.% O_2 in Ar with a flow rate of 200 mL min^{-1}.

Before some of the experiments (catalytic tests, H_2 chemisorption measurements, and IR spectroscopic studies) the passivated samples were reduced in situ with hydrogen at 723 K (for details see below).

Techniques

The nickel content of the catalysts was determined by flame atomic absorption analysis at the resonance wavelength using a PYE-UNICAM SP-1950 apparatus. Supported nickel was dissolved in concentrated nitric acid. Before analysis the solutions were neutralized with ammonia and brought to suitable concentration by dilution with distilled water.

The TEM images were obtained with a JEOL JEM-200 CX transmission electron microscope operating at 200 kV.

Powder XRD patterns were registered at room temperature with a TUR M62 diffractometer using CoKα radiation. The crystallite sizes were calculated from the broadening of the (111) peak fitted to Lorenz curve and using the Scherrer formula [24].

Chemisorption of hydrogen was measured volumetrically in an all-glass device. The chemisorption experiments were performed with passivated samples reduced in situ in hydrogen flow (6 L h^{-1}) at 723 K for 1 h. After reduction as well as after each hydrogen adsorption measurement the samples were evacuated to $P < 1 \times 10^{-3}$ Pa at the temperature of reduction. Adsorption isotherms of hydrogen were obtained in the pressure range 0–13.3 kPa at room temperature. The monolayer coverage was determined by extrapolation of the linear part of the isotherm to zero pressure. It was further used to calculate metal dispersion.

The catalytic experiments were carried out in a flow reactor (0.1 g of the catalyst; particle size of 0.3–0.6 mm) at partial pressure of methanol of 1.57 kPa, WHSV of 0.75 h^{-1}. Methanol dosage was achieved by a saturator thermostated at 273 K using argon as a carrier gas. Two regimes were used: a thermo-programmed regime of heating rate 2 K/min within the temperature range of 400–700 K and isothermal regime at selected temperatures. The gas chromatographic analysis was performed on-line by use of a Polarak Q and molecular sieve 5A columns and ionization and thermoconductivity detectors. The results were calculated using the method of absolute calibration. A carbon-based material balance was done. Before the catalytic test, the samples were pre-treated in situ for 1 h at 723 K in a H_2 flow (6 L h^{-1}) and then cooled down to the reaction temperature in argon.

The FMR measurements were performed with a PS 100 X CentroSpectr (Minsk) spectrometer using 100 kHz modulation of the magnetic field. The g-values were determined with respect to DPPH.

FTIR spectra were recorded with a Nicolet Avatar 360 spectrometer accumulating 64 scans at a spectral resolution of 2 cm^{-1}. Self-supporting pellets (ca 10 mg cm^{-2}) were prepared from the sample powders and treated directly in a purpose-made IR cell allowing measurements at ambient and low temperatures. The cell was connected to a vacuum-adsorption apparatus allowing a residual pressure below 10^{-3} Pa. Prior to adsorption, the samples were reduced in situ by hydrogen (10 kPa) at 723 K and then activated by 1 h outgassing at the same temperature.

Carbon monoxide (>99.5% purity) was supplied by Merck. Before adsorption it was passed through a liquid nitrogen trap.

Results and discussion

Preparation of the samples

Series of samples were prepared by 1–5 successive adsorption–reduction–passivation (SARP) cycles as described in the Experimental part. Figure 1 presents a scheme of the mechanism of this method.

The preparation conditions were chosen on the basis of the earlier investigations with the Ni/SiO_2 system [12, 13]. It was found that grafting of nickel on silica resulted in formation of surface Ni^{2+} species of weak electrophilicity participating in philosilicates of the talk type. These Ni^{2+} species were highly resistant to reduction as elucidated by the temperature-programmed reduction experiment with H_2 up to 1073 K (TPR peak at ca. 956 K). After contact of the reduced samples with synthetic air at room temperature, core–shell particles are formed. The shell represents a new NiO-like phase which can be much easier reduced than the initially deposited nickel (TPR peak at 470 K). This allows reducing the shell of the particles at much lower temperatures than required for the reduction of the initially deposited nickel. Consequently, the authors have chosen a temperature of 723 K for in situ reduction of the passivated samples.

In this study the authors have used a higher concentration of nickel solution (0.3 M Ni^{2+}) as compared to the earlier investigations (0.1 M Ni^{2+}) in order to achieve higher nickel concentration in the samples. It was assumed no significant changes in the state of nickel deposited by the two preparations. Consequently, reduction temperature of 973 K was chosen for preparation of the samples under

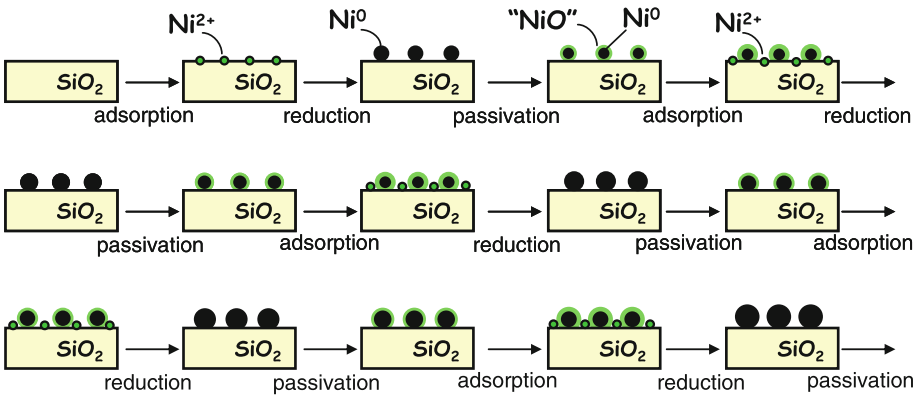

Fig. 1 Scheme of the preparation method of the samples

Table 1 Notation of the samples and some of their characteristics

Sample	Preparation method	Ni content (wt%)	a (μmol H_2 per 1 g of sample)	*D*	S_{sp} (m^2 g^{-1})
Ni-1/SiO_2	One SARP cycle	3.63	68.5	0.22	147.2
Ni-3/SiO_2	Three SARP cycles	7.61	119.7	0.18	123.6
Ni-5/SiO_2	Five SARP cycles	12.62	144.9	0.13	90.2

a quantity of H_2 chemisorbed on 1 g catalyst

D nickel dispersion

S_{sp} specific metal surface area

this study (obtained by 1–5 SARP cycles). To restrict reoxidation of metal particles between the SARP cycles, they were passivated before exposure to air.

Characterization of the samples

Because of their more pronounced difference in concentration, only samples prepared by 1, 3, and 5 SARP cycles have been chosen for further investigation. Their notation and some of their characteristics are summarized in Table 1.

Different techniques giving complementary information were used to characterize the metal particles obtained. Hydrogen chemisorption experiments give the metal dispersion for fully reduced samples, while XRD and FMR results are related to the metal core of the passivated particles. TEM provides information on the size of the whole core–shell particle.

According to the TEM observations, the nickel particles on the Ni-1/SiO_2 sample are uniformly distributed and the size varies between 4 and 5 nm. Uniform particles of around 6 nm were observed on the Ni-3/SiO_2 sample. The largest particles (7 nm) were registered for the Ni-5/SiO_2 sample (Fig. 2). In this case, however, some smaller particles were also detected.

The average metal particle sizes on the passivated samples were also determined by broadening of Ni(111) line in the X-ray diffraction patterns. Figure 3 shows that the Ni(111) line increases in intensity and, at the same time, narrows with the increase of the number of SARP cycles. This is in consistent with the increasing nickel loading and the increasing mean particle size detected by TEM. The data on the mean particle size calculated on the basis of the XRD and TEM results are presented in Table 2.

In order to be able to determine the TOF of the samples in the test reactions, it was measured the metal surface area by H_2 chemisorption (see Table 1). The results showed that the metal-specific surface area and, respectively, the metal

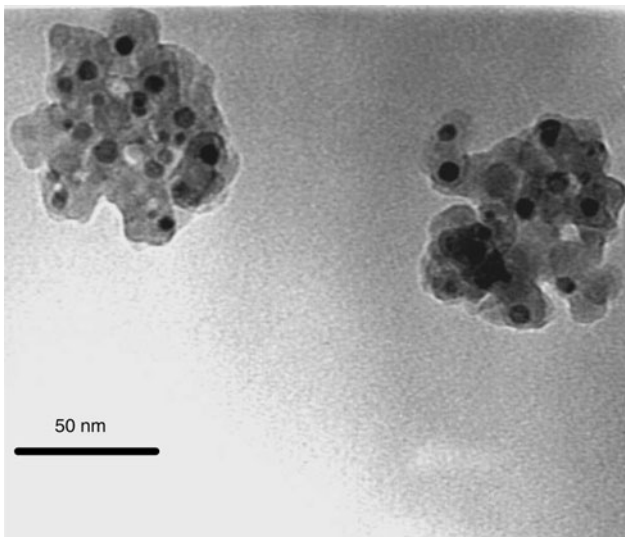

Fig. 2 TEM image of Ni-5/SiO_2

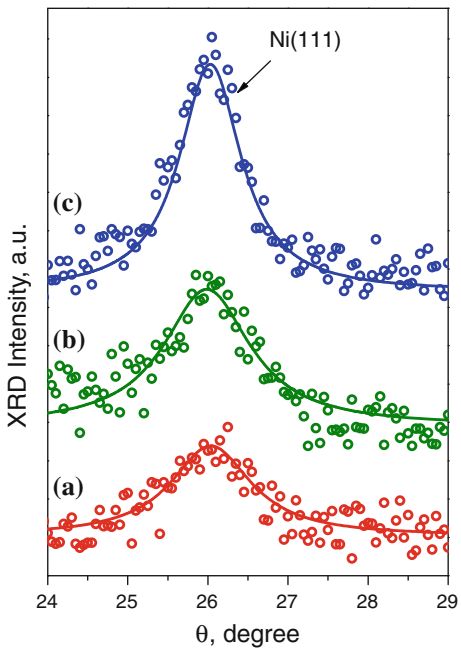

Fig. 3 X-ray diffractograms of the samples: Ni-1/SiO_2 (**a**), Ni-3/SiO_2 (**b**), and Ni-5/SiO_2 (**c**)

Table 2 Mean particle size (nm) determined by different methods

Sample 1	XRD 2	TEM 3	H_2 chemisorption 4	Theoretical[a] 5
Ni-1/SiO_2	4.1	4–5	4.6	–
Ni-3/SiO_2	5.1	6	5.5	5.89
Ni-5/SiO_2	6.1	7	7.5	6.97

[a] For details see text

dispersion, decreased with the increase of the number of SARP cycles (Ni content, respectively). The results are in agreement with the metal particle size increase observed by the other techniques. The particle diameter was calculated on the basis of H_2 chemisorption data assuming the surface stoichiometry of one hydrogen atom per nickel atom, spherical shape of the particles and equal proportions of the three low-index planes (111), (100), and (110) on the their surface [25]. Particle sizes obtained by different methods are summarized in Table 2.

The authors have also calculated the mean particle size for the samples Ni-3/SiO_2 and Ni-5/SiO_2 taking for a base the H_2 chemisorption results concerning the Ni-1/SiO_2 sample. In these calculations it was assumed that (i) each SARP cycle led only to increase of the size of already existing particles and (ii) d^3 (d stands for the mean diameter) was proportional to nickel concentration. Thus, coincidence between the calculated and experimental particle size should indicate that the metal particles produced during the first SARP cycle indeed acted as seeds and each next SARP cycle led mainly to increase in particle size. On the contrary, deviations of the theoretical values from the experimental ones should indicate either increase of the number of metal particles (larger theoretical values) or sintering (smaller theoretical values).

The good coincidence between the theoretical and H_2 chemisorption results for the particle sizes (see Table 1, columns 4 and 5) suggests that the process follows, to a great extent, the Scheme presented in Fig. 1. Small deviations indicate that few new metal particles have been produced, as already observed by TEM.

The characterization by XRD and TEM was performed ex-situ which means that the formed NiO-shell had led to actual decrease of the metal particle size. This effect could not be easily distinguished by TEM but should reflect in the XRD observation. However, the differences between XRD and the hydrogen chemisorption experiments, although observable, were very small. This shows that passivation was efficient and metal particle size was only weakly affected during the exposure of the samples to air.

Ex situ characterization was also performed with ferromagnetic resonance (FMR). This technique can provide information on the dispersion degree of ferromagnetic metals (Ni, Fe, and Co) [2, 26]. A rough estimation of the particle size could be made on the basis of its effect on the FMR line characteristics. The size reduction weakens magnetization and anisotropic effect. As a result, the FMR line shifts, narrows, and becomes less intense [26]. However, for very small clusters with a size of about 1–1.5 nm ("superparamagnetic" particles) the line can appear extremely broad and consequently not observed. Intense broad signals (g factor of about 2.22) typical of nanosized nickel particles were recorded for all the samples. The FMR line (ΔH = 760 G) of the Ni-5/SiO_2 (Fig. 4, spectrum b) is broader as compared to the line (ΔH = 395 G) of Ni-1/SiO_2 (Fig. 4, spectrum a). Thus, these results confirmed that the metal particles on the Ni-5/SiO_2 were larger than those on the parent Ni-1/SiO_2 sample.

FTIR spectra of adsorbed CO

CO is an IR probe molecule that not only allows distinguishing between nickel in different oxidation degrees but also provides details on the state of metal and cationic species [27, 28]. Here the authors shall consider adsorption of CO on reduced Ni/SiO_2 prepared by one SARP cycle (Ni-1/SiO_2, see Table 1). Generally, the results with the other two samples are similar.

Introduction of CO to reduced Ni/SiO_2 at 100 K leads to the appearance of series of bands at 2186, 2156, 2137, 2098, 2052, 2045, 2028, 2002, 1943, and 1897 cm^{-1} (Fig. 5, spectrum a). Upon dynamic vacuum at low temperature the bands above 2130 cm^{-1} disappeared from the spectrum, the stability increasing with the wavenumber (Fig. 5, spectrum b). At the same time, in the region below 2130 cm^{-1}, the doublet at 2052 and 2046 cm^{-1} and the broad band at 1897 cm^{-1} decreased in intensity. The 2098 cm^{-1} band lost some intensity and was gradually

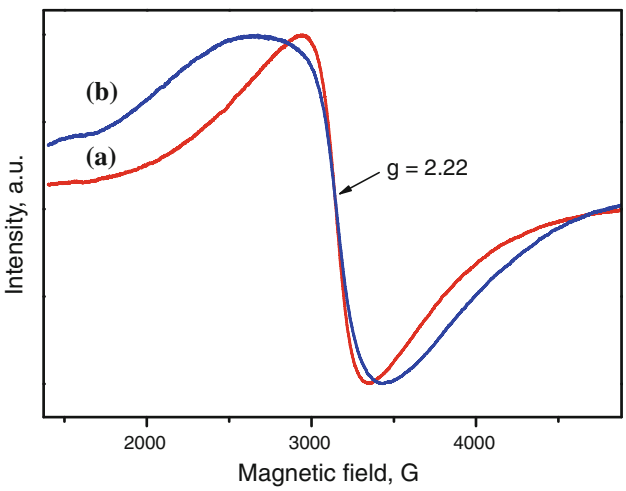

Fig. 4 FMR spectra of the samples: Ni-1/SiO_2 (**a**) and Ni-5/SiO_2 (**b**)

shifted to 2091 cm^{-1}. The weak band at ca 2002 cm^{-1} and a component around 2070 cm^{-1} were the only ones in the spectrum that increased in intensity. Bands at 2129 and 2106 cm^{-1} (shoulder) became clearly visible. At even lower coverages a conversion of a band at 2060 cm^{-1} to a band at 2034 cm^{-1} was observed (Fig. 5, spectrum c and d). Finally, after evacuation at room temperature, only bands at 2034 and 1943 cm^{-1} left in the spectrum (Fig. 5, spectrum d).

The band at 2156 cm^{-1} is due to CO polarized by the silanol groups [28] while the band at 2136 cm^{-1} is attributed to physically adsorbed CO. The band at ca 2186 cm^{-1} is assigned to Ni^{2+}–CO species [12, 13, 28–34]. Its position is rather typical of Ni^{2+} ions from phylosilicates than to Ni^{2+} ions produced after reoxidation of metal nickel. Therefore, the results indicate that small amount of the nickel ions resisted reduction at the experimental conditions applied. It is considered that nickel cations are located at the metal-support interface and act as anchoring sites for the metal particles thus hindering their sintering [2, 7].

All bands in the region 2130–1800 cm^{-1} were registered only with the reduced sample and are thus assigned to different carbonyls formed with reduced nickel sites. The unstable species are different adsorption forms of adsorbed nickel tetracarbonyl (2129, 2106, 2098, 2055, 2046, 2028, and 1897 cm^{-1}) and products of its partial decarbonylation (2070 and 2002 cm^{-1}) [9, 35–37]. Development of the latter bands upon evacuation supports this interpretation. The conversion of the band at 2060 cm^{-1} to the band at 2034 cm^{-1} during coverage decrease is indication that the former one is rather due to dicarbonyls formed on defect metallic sites [35] than to linear CO bonded to Ni^0 sites in vicinity of oxidized phase [38]. The stable species are linear Ni^0–CO (2034 cm^{-1}) and bridged Ni_2^0–CO (2060 cm^{-1}) carbonyls [9, 12, 13, 27, 28, 35, 38].

The formation of nickel tetracarbonyl complicates the system. Some nickel can be removed during the IR experiment which makes the results irreproducible for subsequent CO adsorption experiments. In addition, tetracarbonyl formation can play a role in catalytic processes (removal of Ni, changing size, and morphology of the Ni particles) with the participation of CO as a reactant or product [2, 35]. Note that formation of nickel tetracarbonyl occurs with small metal particles and the process is favoured by high-CO equilibrium pressure and low temperature [35]. Consequently, formation of nickel tetracarbonyl during the catalytic reaction could be expected with methanol decomposition at low temperatures and, above all, with the Ni-1/SiO_2 sample.

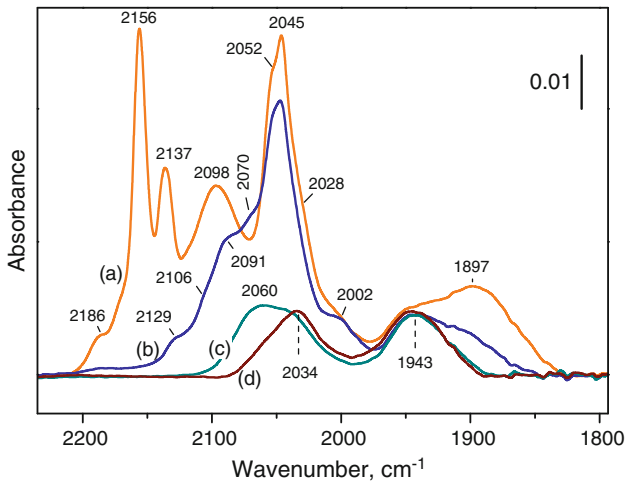

Fig. 5 IR spectra taken after CO adsorption at 100 K on Ni-1/SiO_2. Initial equilibrium pressure of 200 Pa and evolution of the spectra under dynamic vacuum at 100 K (**a**, **b**) and at increasing temperature (**c**, **d**)

Methanol decomposition

The methanol decomposition test was carried out at three-different temperatures (476, 500, and 511 K). Note that it was observed the secondary interaction between CO and H_2 (to produce CH_4) practically at $T > 515$ K. It is seen from Fig. 6a that the total activity of the catalysts passes through a maximum, i.e., the highest activity is manifested by Ni-3/SiO_2, irrespective of the lower nickel concentration as compared to Ni-5/SiO_2. In addition, the catalytic activity was stable which indicated (i) no measurable effect of eventual formation of nickel tetracarbonyl and (ii) no blocking of the catalytically active sites by carbonaceous deposit.

Figure 6b shows the TOF manifested by the different catalysts. TOF represents methanol molecules converted per surface nickel atom per unit time and was calculated using the following formula:

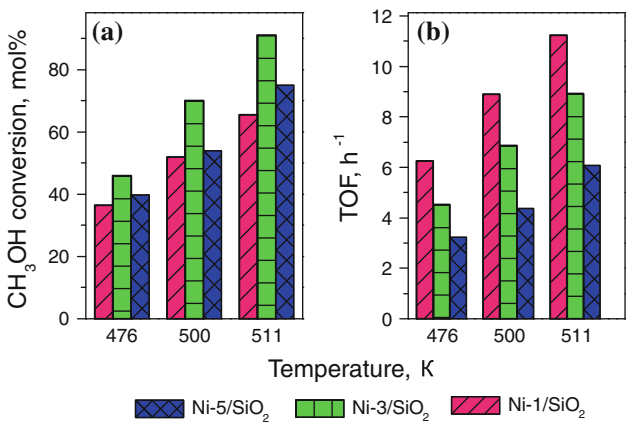

Fig. 6 Methanol conversion to CO and H_2 (**a**) and corresponding TOF (**b**) on Ni-1/SiO_2, Ni-3/SiO_2, and Ni-5/SiO_2 at different temperatures

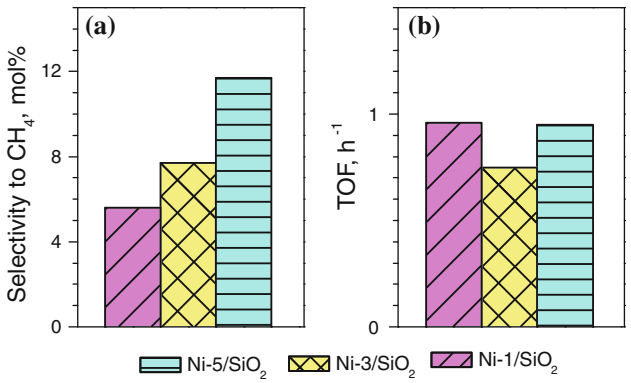

Fig. 7 Selectivity to methane at 520 K on Ni-1/SiO_2, Ni-3/SiO_2, and Ni-5/SiO_2 (**a**) and corresponding TOF (**b**)

$$TOF = \frac{sx}{nma}$$

where *TOF* is the turn-over frequency (h^{-1}), *s*, methanol weight velocity (mol h^{-1}); *x,* methanol conversion (mol/mol); *m,* the mass of the sample (g); *a,* the hydrogen uptake on the catalyst (mol H_2 per 1 g sample); *n,* the chemisorption stoichiometry representing the average number of surface metal atoms associated with the adsorption of each gas molecule at monolayer coverage ($n = Ni_s/H_2 = 2$).

It is clearly seen that TOF decreases with increase of nickel loading. These results unambiguously demonstrate that methanol decomposition to CO and H_2 is a structure sensitive reaction. The fact that TOF decreases with the increase of metal particle size in the range between 4 and 7 nm could be linked to the role of low-coordination sites at edges and corners. However, Matrsumura et al. [16, 17] reported that catalysts containing small nickel particles, with a size of 2–4 nm, were with low efficiency. This suggests that the catalytic reaction could require an optimal particle diameter at around 4 nm. Indeed, for a number of reactions the dependence of TOF on *d* passes trough a maximum in the range about 2–3 nm [2]. Usually this was explained by the existence of special sites (e.g., the so-called B_5 sites near edges). Alternatively, the authors could suggest that very small particles interact readily with CO to form nickel tetracarbonyl which reflects in a low efficiency of the catalysts.

Catalytic experiments were also performed at temperatures higher than 515 K in order to obtain information on the performance of the samples in the CO methanation reaction. Although the results are more difficult to interpret because of the occurrence of two subsequent reactions, the dependencies presented in Fig. 7 indicate that, in the framework of the experimental error, this reaction is structure insensitive. This finding is consistent with many literature data [21, 22] pointing out that CO methanation is a structure insensitive reaction.

Finally, the authors would like to note that the proposed by us preparation technique appears to be convenient for synthesis of catalyst with pre-set metal particle size. In addition, it is suitable for studying structure sensitivity because eliminates the effect of preparation and is thus complementary to the approach used by Hou et al. [5, 6] who kept the same nickel loading for catalysts prepared using different precursors.

Conclusions

- Successive adsorption–reduction–passivation is a promising method for preparation of silica-supported nickel nanoparticles with increasing metal concentration and particle size.
- Methanol decomposition on Ni/SiO_2 catalysts is characterized by structure sensitivity and TOF of the catalysts decreases with particle size increase when they range from 4 to 7 nm.
- CO methanation on Ni/SiO_2 catalysts seems to be structure insensitive reaction.

Acknowledgments This study was supported by the Bulgarian Scientific Fund (Grants 02-290/2008 and DCVP 02/2009). The authors thank Dr. M. Shopska for her assistance with the H_2 chemisorption measurements.

References

1. Bond GC (2003) In: Cornils B, Herrmann WA, Slögl R, Wong C-H (eds) Catalysis from A to Z, 2nd edn. Wiley–VCH, Weinheim, p 728
2. Che M, Bennett CO (1989) Adv Catal 38:55
3. Dumesic JA, George WH, Boudart M (2008) In: Ertl G, Knözinger H, Schüth F, Weitkamp J (eds) Handbook of heterogeneous catalysis, 2nd edn. Wiley VCH, Weinheim, p 1446
4. Heiz U, Landman U (eds) (2007) Nanocatalysis. Springer, New York
5. Hou Z, Gao J, Guo J, Liang D, Lou H, Zheng X (2007) J Catal 250:331
6. Guo J, Hou Z, Gao J, Zheng X (2008) Energy Fuel 22:1444
7. Marceau E, Carrier X, Che M, Clause O, Marcilly C (2008) In: Ertl G, Knözinger H, Schüth F, Weitkamp J (eds) Handbook of heterogeneous catalysis, 2nd edn. Wiley VCH, Weinheim, p 467
8. Schwarz JA, Contescu C, Contescu A (1995) Chem Rev 95:477
9. Hadjiivanov K, Mihaylov M, Abadjieva N, Klissurski D (1998) J Chem Soc Faraday Trans 94:3711
10. Hadjiivanov K, Saint-Just J, Che M, Tatibouet J-M, Lamotte J, Lavalley JC (1994) J Chem Soc Faraday Trans 90:2277
11. Haller GL, Resasco DE (1989) Adv Catal 36:173
12. Hadjiivanov K, Mihaylov M, Klissurski D, Stefanov P, Abadjieva N, Vassileva E, Mintchev L (1999) J Catal 185:314
13. Mihaylov M, Hadjiivanov K, Klissurski D (2000) In: Proceedings of IX international symposium heterogeneous catalysis, Varna, p 387
14. Agrell J, Lindstroem B, Pettersson LJ, Jaras S (2002) In: Spivey JJ (ed) Catalysis, vol 16. Royal Society of Chemistry, Cambridge, p 272

15. Navarro RM, Peňa MA, Fierro JLG (2007) Chem Rev 107:3952
16. Matsumura Y, Tanaka K, Tode N, Yazawa T, Haruta M (2000) J Mol Catal A 152:157
17. Matsumura Y, Tode N (2001) Phys Chem Chem Phys 3:1284
18. Eigenberger G (2008) In: Ertl G, Knözinger H, Schüth F, Weitkamp J (eds) Handbook of heterogeneous catalysis, 2nd edn. Wiley VCH, Weinheim, p 2085
19. Harms A, Høhlein B, Jørn E, Skov A (1980) Oil Gas J 78:120
20. Dry M (2004) Appl Catal A Gen 276:1
21. Goodman JG Jr, Kim S, Rhodes WD (2004) In: Spivey JJ (ed) Catalysis, vol 17. Royal Society of Chemistry, Cambridge, p 326
22. Kelley RD, Goodman DW (1982) In: King DA, Woodruff DP (eds) Chemical physics of solid surface and heterogeneous catalysis, vol 4. Elsevier, Amsterdam, p 427
23. Rostrup-Nielsen JR, Pedersen K, Sehested J (2007) Appl Catal A Gen 330:134
24. Andersson MP, Abild-Pedersena F, Remediakis IN, Bligaard T, Jones G, Engbæk J, Lytken O, Horcha S, Nielsenb JH, Sehested J, Rostrup-Nielsen JR, Nørskov JK, Chorkendorff I (2008) J Catal 255:6
25. Bergeret G, Gallezot P (2008) In: Ertl G, Knözinger H, Schüth F, Weitkamp J (eds) Handbook of heterogeneous catalysis, 2nd edn. Wiley VCH, Weinheim, p 738
26. Slinkin AA (1968) Usp Khim 37:1521
27. Davydov AA (2003) In: Sheppard NT (ed) Molecular spectroscopy of oxide catalyst surfaces. Wiley, Chichester
28. Hadjiivanov K, Vayssilov G (2002) Adv Catal 47:307
29. Hadjiivanov K, Knözinger H, Mihaylov M (2002) J Phys Chem B 106:2618
30. Penkova A, Dzwigaj S, Kefirov R, Hadjiivanov K, Che M (2007) J Phys Chem C 111:8623
31. Hierl R, Knözinger H (1981) J Catal 69:475
32. Duchet JC, Lavalley JC, Housni S, Ouafi D, Bachelier J, Lakhdar M, Mennour M, Cornet D (1988) Catal Today 4:71
33. Anderson JA, Daza L, Fierro JLG, Rodrigo MT (1993) J Chem Soc Faraday Trans 89:3651
34. Borello E, Cimino A, Ghiotti G, Jacono ML, Schiavello M, Zecchina A (1971) Discuss Faraday Soc 52:149
35. Mihaylov M, Hadjiivanov K, Knözinger H (2001) Catal Lett 76:59
36. Mohana Rao K, Spoto G, Zecchina A (1989) Langmuir 5:319
37. Wendland K-P, Bremer H, Vogt F, Reshitlovski WP, Mörke W, Hobert H, Weber M, Becker K (1987) Appl Catal 31:65
38. Sheppard N, Nguyen TT (1978) In: Clarke PJ, Hester RE (eds) Advances in Infrared and Raman Spectroscopy, vol. 5. Wiley, New York, p 67